Application of the Arlequin method to some structures with defects

Hachmi Ben Dhia, Guillaume Rateau

Application of the Arlequin method to some structures with defects

Hachmi Ben Dhia[*]– **Guillaume Rateau**[**]

* *Laboratoire MSS-Mat, Unité Mixte de Recherche 8579 CNRS*
École Centrale Paris, Châtenay-Malabry, France
bendhia@mss.ecp.fr

** *Département Mécanique et Modèles Numériques*
Direction d'Étude et Recherche EdF, Clamart, France
guillaume.rateau@edf.fr

ABSTRACT. *The Arlequin method offers an alternative framework for the multimodel mechanical simulations. This paper aims at showing the promising potentialities of this approach to introduce defects in a sound model with great flexibility. The formulations and the related theoretical results are recalled and the key points for numerical implementation are discussed. Numerical examples illustrate their efficiency.*

RÉSUMÉ. *La méthode Arlequin offre un cadre de modélisation alternatif pour la simulation de problèmes mécaniques multimodèles. Dans cet article, nous montrons les potentialités importantes de cette méthode pour introduire des défauts dans un modèle sain avec une grande flexibilité. Nous rappelons les principes et le cadre d'application de la méthode et nous discutons sa mise en œuvre informatique. Des résultats numériques éclairent notre démarche et témoignent de la pertinence de l'approche.*

KEYWORDS: *defects, Arlequin method, numerical aspects, applications.*

MOTS-CLÉS : *défauts, méthode Arlequin, aspects numériques, applications.*

1. Introduction

Solving mechanical problems with defects (such as cracks or inclusions) is essential in the designing or the maintaining of large structures. The main difficulty lies in the discrepancy between the scale of the defects and the structure. In finite element methods, this requires specially refined meshes. Such meshes must be generated for each distribution of defects and the generation of one of them is almost always a time-consuming and tedious task.

This concern is akin to a more general one : multiscale mechanical problems. In the past few years, many approaches based on the same ideas have been designed. In those methods (eg. [Bab 00, Hug 98, Lad 99, Ode 97, Suk 97]), the structure is coarsely meshed and special correction terms are added to the finite element functions basis. In a word, the approximation space is enlarged by summing vector spaces.

An alternative strategy lies in substituting a product for this sum; it results in the *Arlequin* method [Ben 98, Ben 99]. It is based on three ideas. (I_1) The core idea is to superpose several mechanical states in some zones of the material system. (I_2) The superposition lies then in the global formulation by making the virtual works be shared by the different states thanks to weight parameter functions. (I_3) In order to link the superposed models together, fictive forces are activated to weakly control the deviation between the respective fields of the models, in parts of the overlapping zones (called *glue zones*).

Arlequin is thus a general method to glue one model to another one. Therefore by superposing models, three different modelling actions can be combined (see fig. 1): (A_1) superposing to locally refine models (zoom), (A_2) superposing to link structure models and (A_3) superposing to alter models locally by means of an *internal junction*.

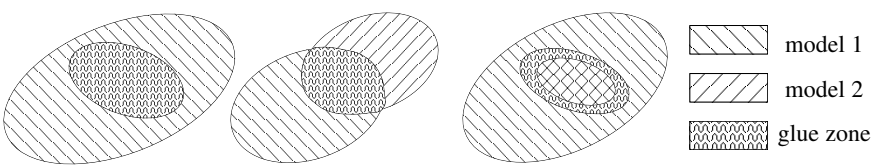

Figure 1. *Modelling actions*

In this paper, we will focus on the use of this third modelling action and show how it can be used to quickly and easily add defects or inclusions in a sound model.

The outline is the following. We first recall the continuous and the discrete mixed *Arlequin* equations for a model elasticity problem and some theoretical results stating the well-posedness of those formulations [Ben 01b, Ben 01a]. In the section 3, the discretisation by the finite element method and the related implementation concern are described. Finally numerical results showing the efficiency of the method are presented in section 4 for relevant mechanical examples.

2. Arlequin formulations and mathematical results

The *Arlequin* formulations [Ben 98] and the mathematical results established in [Ben 01b] are recalled for completeness of purpose.

2.1. *Continuous Formulation*

We consider a static bi-dimensional linearized elasticity problem defined in a polygonal domain Ω. We let Γ, $\boldsymbol{f}$, ε and $\boldsymbol{\sigma}$ respectively denote the clamped part of the boundary $\partial\Omega$, the applied density of surface forces, the linearized strain and stress tensors. We assume that the constitutive material law is a Hooke one:

$$\boldsymbol{\sigma}_{ij} = \boldsymbol{R}_{ijkl}\,\boldsymbol{\varepsilon}_{kl} \qquad [1]$$

The elasticity moduli $\boldsymbol{R}_{ijkl}$ are assumed to satisfy the following classical symmetry, coercitivity and regularity hypotheses (usual conventions of summation over repeated indices are used):

$$\boldsymbol{R}_{ijkl} = \boldsymbol{R}_{jikl} = \boldsymbol{R}_{klij} \qquad [2]$$

$$\exists\, c_0 > 0\ ; \quad \boldsymbol{R}_{ijkl}\,\boldsymbol{\tau}_{ij}\boldsymbol{\tau}_{kl} \geq c_0\,\boldsymbol{\tau}_{ij}\boldsymbol{\tau}_{ij}, \qquad \forall\, \boldsymbol{\tau}_{ij} = \boldsymbol{\tau}_{ji} \qquad [3]$$

$$\boldsymbol{R}_{ijkl} \in L^{\infty}(\Omega) \qquad [4]$$

The classical displacement problem then reads as follows:

$$\min_{\boldsymbol{v}\in\boldsymbol{W}} e(\boldsymbol{v}) \qquad [5]$$

$$\boldsymbol{W} = \{\boldsymbol{v} \in \boldsymbol{H}^1(\Omega)\ ;\ \boldsymbol{v} = \boldsymbol{0} \text{ on } \Gamma\} \qquad [6]$$

$$e(\boldsymbol{v}) = \tfrac{1}{2}a(\boldsymbol{v},\boldsymbol{v}) - b(\boldsymbol{v}) \qquad [7]$$

$$a(\boldsymbol{u},\boldsymbol{v}) = \int_\Omega \boldsymbol{\sigma}(\boldsymbol{u}) : \varepsilon(\boldsymbol{v})\, d\Omega \qquad [8]$$

$$b(\boldsymbol{v}) = \int_\Omega \boldsymbol{f}.\boldsymbol{v}\, d\Omega \qquad [9]$$

$$\boldsymbol{\epsilon}_{i\,j}(\boldsymbol{u}) = \tfrac{1}{2}(\partial_j \boldsymbol{u}_i + \partial_i \boldsymbol{u}_j) \qquad [10]$$

To rewrite this problem according to the *Arlequin* method, we consider that Ω is covered by two overlapping polygonal domains Ω_1 and Ω_2. The clamped part Γ is

assumed to be, say, in $\partial\Omega_1$. We let Ω_M denote the glue zone supposed to be a non zero measured polygonal subset of $\Omega_1 \cap \Omega_2$ (see fig. 2).

To model the gluing forces, we use the choice suggested in [Ben 98] and analysed in [Ben 01b]. Thus those forces are modelled as Lagrange multipliers belonging to the functional space $\boldsymbol{W}_M = \boldsymbol{H}^1(\Omega_M)$ called *mediator*.

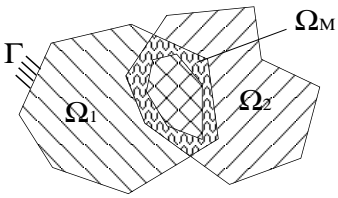

Figure 2. *Superposed models and the glue zone*

In this way, the problem can be rewritten as the following saddle-point variational principle:

$$\min_{(\boldsymbol{v}_1,\boldsymbol{v}_2)\in \boldsymbol{W}_1\times\boldsymbol{W}_2} \max_{\boldsymbol{\lambda}\in\boldsymbol{W}_M} \{e_1(\boldsymbol{v}_1) + e_2(\boldsymbol{v}_2) + c(\boldsymbol{\lambda}, \boldsymbol{v}_1 - \boldsymbol{v}_2)\} \quad [11]$$

$$\boldsymbol{W}_1 = \{\boldsymbol{v}_1 \in \boldsymbol{H}^1(\Omega_1) \ ; \ \boldsymbol{v}_1 = \boldsymbol{0} \text{ on } \Gamma\} \quad [12]$$

$$\boldsymbol{W}_2 = \boldsymbol{H}^1(\Omega_2) \quad [13]$$

$$\boldsymbol{W}_M = \boldsymbol{H}^1(\Omega_M) \quad [14]$$

$$e_i(\boldsymbol{v}_i) = \tfrac{1}{2} a_i(\boldsymbol{v}_i, \boldsymbol{v}_i) - b_i(\boldsymbol{v}_i) \quad [15]$$

$$a_i(\boldsymbol{u}_i, \boldsymbol{v}_i) = \int_{\Omega_i} \alpha_i \, \boldsymbol{\sigma}(\boldsymbol{u}_i) : \boldsymbol{\varepsilon}(\boldsymbol{v}_i) \, d\Omega \quad [16]$$

$$b_i(\boldsymbol{v}_i) = \int_{\Omega_i} \beta_i \, \boldsymbol{f}.\boldsymbol{v}_i \, d\Omega \quad [17]$$

$$c(\boldsymbol{\lambda}, \boldsymbol{v}) = \int_{\Omega_M} (\boldsymbol{\lambda}.\boldsymbol{v} \ + \kappa \boldsymbol{\nabla}\boldsymbol{\lambda} : \boldsymbol{\nabla}\boldsymbol{v}) \, d\Omega \quad [18]$$

where α_i, β_i and κ respectively denote two weight parameter functions and a strictly positive adimensional parameter.

The weight parameter functions α_i and β_i are required not to count the energy in the overlap twice. Therefore they are assumed to be positive piecewise continuous functions in Ω_i and to satisfy the following equalities:

$$\alpha_1 + \alpha_2 = \beta_1 + \beta_2 = 1 \qquad \text{in} \quad \Omega_1 \cap \Omega_2 \quad [19]$$

$$\alpha_i = \beta_i = 1 \qquad \text{in} \quad \Omega_i \setminus (\Omega_1 \cap \Omega_2) \quad [20]$$

2.2. *Discrete formulations*

The discrete formulations are derived from the continuous one by means of the finite element method. To this end, for i varying in the set $\{1, 2, M\}$, we consider

triangulations of Ω_i, denoted (T_{h_i}). We let $\boldsymbol{W}_i^h \subset \boldsymbol{W}_i$ denote the related conforming finite element spaces. Then the discrete problem reads:

$$\min_{(\boldsymbol{v}_1^h, \boldsymbol{v}_2^h) \in \boldsymbol{W}_1^h \times \boldsymbol{W}_2^h} \max_{\boldsymbol{\lambda}^h \in \boldsymbol{W}_M^h} e_1(\boldsymbol{v}_1^h) + e_2(\boldsymbol{v}_2^h) + c(\boldsymbol{\lambda}^h, \boldsymbol{v}_1^h - \boldsymbol{v}_2^h) \qquad [21]$$

The Euler equations are then derived from [21]. They read :

$$\text{Find } (\boldsymbol{u}_1^h, \boldsymbol{u}_2^h, \boldsymbol{\lambda}^h) \in \boldsymbol{W}_1^h \times \boldsymbol{W}_2^h \times \boldsymbol{W}_M^h ; \forall\, (\boldsymbol{v}_1^h, \boldsymbol{v}_2^h, \boldsymbol{\mu}^h) \in \boldsymbol{W}_1^h \times \boldsymbol{W}_2^h \times \boldsymbol{W}_M^h,$$

$$a_1(\boldsymbol{u}_1^h, \boldsymbol{v}_1^h) = b_1(\boldsymbol{v}_1^h) - c(\boldsymbol{\lambda}^h, \boldsymbol{v}_1^h) \qquad [22]$$

$$a_2(\boldsymbol{u}_2^h, \boldsymbol{v}_2^h) = b_2(\boldsymbol{v}_2^h) + c(\boldsymbol{\lambda}^h, \boldsymbol{v}_2^h) \qquad [23]$$

$$c(\boldsymbol{\mu}^h, \boldsymbol{u}_1^h) = c(\boldsymbol{\mu}^h, \boldsymbol{u}_2^h) \qquad [24]$$

Note that in [22] and [23], the second member of the right hand side terms stands for the virtual work of the junction forces and that [24] is the weak junction system.

2.3. *Mathematical results*

In [Ben 01b], we established the following theorems. They state that, under conditions which are easy to satisfy, the continuous and the discrete problems are well-posed. We let denote $\boldsymbol{W}_{|A} = \{\boldsymbol{v}_{|A}\, ;\, \boldsymbol{v} \in \boldsymbol{W}\}$. The natural norm of the space $\boldsymbol{A}$ and the greater diameter of the triangles in the triangulation (T_{h_i}) are denoted by $\|.\|_{\boldsymbol{A}}$ and h_i, respectively.

Theorem 1 .
Under the hypotheses [2]-[4] for the elasticity moduli and [19]-[20] for the weight paramater functions. If

$$\forall i \in \{1,2\},\ \exists\, \alpha_{0_i} > 0\ ;\ \alpha_i \geq \alpha_{0_i}\ in\, \Omega_1 \cap \Omega_2 \qquad [25]$$

Then the continuous problem [1], [10], [11]-[18] admits a unique solution $(\boldsymbol{u}_1, \boldsymbol{u}_2, \boldsymbol{\lambda})$ *in* $\boldsymbol{W}_1 \times \boldsymbol{W}_2 \times \boldsymbol{W}_M$.

Theorem 2 .
Under the hypotheses [2]-[4] for the elasticity moduli and [19]-[20], [25] for the weight paramater functions. Assume that the triangulations (T_{h_1}), (T_{h_2}) *and* (T_{h_M}) *are regular enough to use interpolation theory and inverse inequalities [Cia 78]. If, in addition,*

$$\boldsymbol{W}_M^h \subset \boldsymbol{W}_{1\,|\Omega_M}^h \quad or \quad \boldsymbol{W}_M^h \subset \boldsymbol{W}_{2\,|\Omega_M}^h \qquad [26]$$

Then the discrete problem [1], [10], [15]-[18], [21] admits a unique solution $(\boldsymbol{u}_1^h, \boldsymbol{u}_2^h, \boldsymbol{\lambda}^h)$ *in* $\boldsymbol{W}_1^h \times \boldsymbol{W}_2^h \times \boldsymbol{W}_M^h$.

Theorem 3 .
Under the hypotheses of Theorem 2, the solution of the continuous and discrete problems satisfy an optimal a priori error estimate.
If $\boldsymbol{u}_1 \in \boldsymbol{W}_1 \cap \boldsymbol{H}^2(\Omega_1)$, $\boldsymbol{u}_2 \in \boldsymbol{W}_2 \cap \boldsymbol{H}^2(\Omega_2)$ *and* $\boldsymbol{\lambda} \in \boldsymbol{W}_M \cap \boldsymbol{H}^2(\Omega_M)$, *then :*

$$\exists\, C > 0 \text{ indepedent of } h_1,\ h_2 \text{ and } h_M \ ;$$

$$\|\boldsymbol{u}_1 - \boldsymbol{u}_1^h\|_{\boldsymbol{W}_1} + \|\boldsymbol{u}_2 - \boldsymbol{u}_2^h\|_{\boldsymbol{W}_2} + \|\boldsymbol{\lambda} - \boldsymbol{\lambda}^h\|_{\boldsymbol{W}_M} \leq C \max(h_1, h_2, h_M) \quad [27]$$

Theorem 1 results in the identity between the restriction to Ω_1 and Ω_2 of the solution $\boldsymbol{u}$ of problem [5] and $(\boldsymbol{u}_1,\ \boldsymbol{u}_2)$ of problem [11], since $(\boldsymbol{u}_1, \boldsymbol{u}_2)$ is unique and $(\boldsymbol{u}_{|\Omega_1},\ \boldsymbol{u}_{|\Omega_2})$ satisfies the equilibrium equations related to [11]. The inequality [27] establishes that, in the worst case, the discretization error is controlled by the step of the coarser triangulation.

We will see in subsection 3.1 that the condition [25] on the weight parameter functions α_i presents no pratical difficulty. In addition, the compatibility condition [26] can rather easily be satisfied in pratice. Indeed the triangulation (T_{h_M}) can be chosen as the restriction to Ω_M of (T_{h_1}) or (T_{h_2}). This choice has an influence on the solution as the numerical example 4.1 in [Ben 01a] shows. This question, related to the compatibility of the motion of models is now being studied in an enlarged framework by the first author of this paper and will be tested for the particular case of the *Arlequin* approach.

3. Implementation issue

This section is adressed to the key points for the numerical implementation of the *Arlequin* method, namely how to numerically represent the weight parameter functions, then how to choose them, what is the linear system and how to cope with the incompatibility of models.

3.1. *Numerical representation of the weight parameter functions*

When a generalised heterogeneous superposition of N models is considered, the conditions [19]-[20] show that the weight parameter functions must be defined by pieces. Therefore we first focus on these pieces. To this end, we index the subdomains related to each model by Ω_1, Ω_2 ... Ω_N. Denoting by P_N the set of parts which can be constituted with the N indices $1 \ldots N$, a partition of the domain Ω (see fig. 3a) is obtained by considering the following subdomains called *elementary subdomains*:

$$\forall\, I \in P_N,\ \Theta_I = (\mathop{\cap}_{i \in I} \Omega_i) \setminus (\mathop{\cup}_{j \notin I} \Omega_j) \text{ when } \Theta_I \neq \emptyset \quad [28]$$

These elementary subdomains make up the pieces on which the weight parameter functions must be defined and indeed an easy way to satisfy [19]-[20] consists in

gathering in each Θ_I, the weight parameter functions α_i and β_i in vector fields denoted by $\boldsymbol{\alpha}$ and $\boldsymbol{\beta}$ defined as follows. At a point $\boldsymbol{x}$ in Θ_I, the field, say, $\boldsymbol{\alpha}$ is equal to $(\alpha_{i_1}(\boldsymbol{x}) \ldots \alpha_{i_k}(\boldsymbol{x}))$ where $\{i_1, \ldots, i_k\} = I$. The generalised conditions [19]-[20] are then simply rewritten as follows :

$$\forall\, I = \{i_1, \ldots, i_k\} \in P_N,\ \textstyle\sum_{j=1}^{k} \alpha_{i_j} = 1 \text{ in } \Theta_I \qquad [29]$$

For instance, in figure 2, $\boldsymbol{\alpha}$ corresponds to (α_1, α_2) in $\Theta_{\{1,2\}} = \Omega_1 \cap \Omega_2$ and to (α_i) in $\Theta_{\{i\}} = \Omega_i \setminus (\Omega_1 \cap \Omega_2)$. The equation [28] results in $\alpha_1 + \alpha_2 = 1$ in $\Theta_{\{1,2\}}$ and $\alpha_i = 1$ in $\Theta_{\{i\}}$.

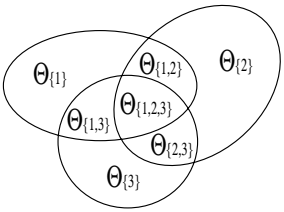

Figure 3a. *Subdomains* Θ_I

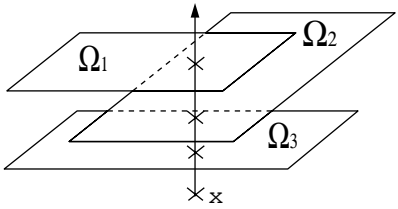

Figure 3b. *Association between* $\boldsymbol{x}$ *and* Θ_I

If we assume that the functions α_i and β_i are continuous in the elementary subdomains Θ_I, the fields $\boldsymbol{\alpha}$ and $\boldsymbol{\beta}$ can be discretized over a finite element space. Nonetheless, given the definition of these fields, this space must be generated by independent triangulations of Θ_I. We have thus chosen the easiest representation consisting in taking $\boldsymbol{\alpha}$ and $\boldsymbol{\beta}$ as vector-valued fields which are constant in each elementary subdomain.

Since $\{\Theta_I\}$ stands for a partition of the domain Ω, each point $\boldsymbol{x}$ in Ω can be associated with a Θ_I (except in some boundaries for which a choice is automatically made). Numerically this association can be achieved in finding the list of subdomains $(\Omega_{i_1} \ldots \Omega_{i_k})$ in which $\boldsymbol{x}$ is located (see fig. 3b, where, for clarity, the subdomains have been translated).

3.2. *Choice of the weight parameter functions* α_i

The weight parameter functions α_i are assumed to be given. The *optimal* choice seems to be a rather intricate question. A heuristic one consists then in relating α_i to the relative finess of the associated model. The limit case is obtained when one model is only consitituted of rigid body motions. Since the internal energy is then equal to zero, the associated weight parameter function must be null. In this way, we recover the method developed by Glowinski et al. [Glo 00], called *fictitious domain method with a distributed Lagrange multiplier* (whose applications to fluid/rigid coupling problem are quite important). A use of the *Arlequin* framework for fluid / solid coupling is a work in progress.

3.3. *Linear system*

We now focus on the linear system to solve. For the sake of simplicity, we consider that only two models are superposed. We let $(\boldsymbol{w}_i^1)$, $(\boldsymbol{w}_j^2)$ and $(\boldsymbol{w}_k^M)$ denote the finite element basis functions of $\boldsymbol{W}_1^h$, $\boldsymbol{W}_2^h$ and $\boldsymbol{W}_M^h$, respectively. The vectors $[\mathrm{U}_1]$, $[\mathrm{U}_2]$ and $[\Lambda]$ stand respectively for the coordinates of $\boldsymbol{u}_1$, $\boldsymbol{u}_2$ and $\boldsymbol{\lambda}$ in those bases. The linear system reads :

$$\begin{bmatrix} \mathrm{K}_1 & & \mathrm{B}_1 \\ & \mathrm{K}_2 & -\mathrm{B}_2 \\ \mathrm{B}_1^T & -\mathrm{B}_2^T & \end{bmatrix} \begin{bmatrix} \mathrm{U}_1 \\ \mathrm{U}_2 \\ \Lambda \end{bmatrix} = \begin{bmatrix} \mathrm{F}_1 \\ \mathrm{F}_2 \\ 0 \end{bmatrix} \qquad [30]$$

$$[\mathrm{K}_i]_{j\,k} = \int_{\Omega_i} \alpha_i\, \boldsymbol{\sigma}(\boldsymbol{w}_j^i) : \boldsymbol{\varepsilon}(\boldsymbol{w}_k^i)\, d\Omega \qquad [31]$$

$$[\mathrm{B}_i]_{j\,k} = \int_{\Omega_M} \boldsymbol{w}_j^M . \boldsymbol{w}_k^i \; + \kappa \boldsymbol{\nabla} \boldsymbol{w}_j^M : \boldsymbol{\nabla} \boldsymbol{w}_k^i \, d\Omega \qquad [32]$$

$$[\mathrm{F}_i]_j = \int_{\Omega_i} \beta_i\, \boldsymbol{f} . \boldsymbol{w}_j^i \, d\Omega \qquad [33]$$

Note that there are two kinds of matrices, namely the rigidity matrices $[\mathrm{K}_i]$ and the coupling matrices $[\mathrm{B}_i]$ related to the junction operator.

The computation of the rigidity matrices $[\mathrm{K}_i]$ and the force vector $[\mathrm{F}_i]$ is achieved by classically assembling, for each K in (T_{h_1}) or (T_{h_2}) the elementary rigidity matrices $[\mathrm{K}_i^K]$ and force vectors $[\mathrm{F}_i^K]$.

$$\left[\mathrm{K}_i^K\right]_{j\,k} = \int_K \alpha_i\, \boldsymbol{\sigma}(\boldsymbol{w}_j^i) : \boldsymbol{\varepsilon}(\boldsymbol{w}_k^i)\, d\Omega \qquad [34]$$

$$\left[\mathrm{F}_i^K\right]_j = \int_K \beta_i\, \boldsymbol{f} . \boldsymbol{w}_j^i \, d\Omega \qquad [35]$$

j, k degrees of freedom of K

On the other hand, the computation of the coupling matrices $[\mathrm{B}_i]$ is completed in the following way. We first pair the mediator with the models. Namely, for each triangle K in (T_{h_M}), the lists (L_i^K) of triangles in (T_{h_i}) facing K are computed. The coupling matrices are then made up by assembling the elementary coupling matrices $[\mathrm{B}_i^{K\,L}]$.

$$\forall\, K \in (T_{h_M}),\ L \in (L_i^K),$$

$$\left[\mathrm{B}_i^{K\,L}\right]_{j\,k} = \int_{K\cap L} \boldsymbol{w}_j^M . \boldsymbol{w}_k^i \; + \kappa \boldsymbol{\nabla} \boldsymbol{w}_j^M : \boldsymbol{\nabla} \boldsymbol{w}_k^i \, d\Omega \qquad [36]$$

j, k degrees of freedom of K and L, respectively

Note that algebraically the triangles K and L play the same role in the integral [36]. Therefore, this integral can be computed either on the restriction of K to L or the restriction of L to K.

3.4. *Incompatibility and hierarchical quadrature*

The *Arlequin* method presents no a priori restriction on the way the models are superposed. In particular, there is no restriction about the location of the nodes or the boundaries of one model with regard to another. Nevertheless this convenience results in inhomogeneities in the integrals [34]-[36] and the numerical integration must be more sophisticated. We focus on the computation of $[\mathrm{K}_1]$, $[\mathrm{F}_1]$ and $[\mathrm{B}_1]$.

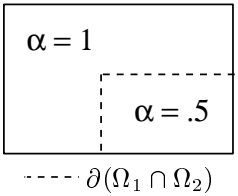

Figure 4a. *Inhomogeneous* α

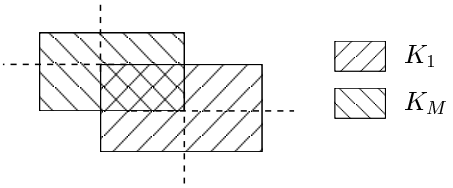

Figure 4b. *Inhomogeneous coupling*

Given the chosen way to numerically represent the weight parameter functions, the computation of [34]-[35] may be unusual. Indeed, if there exists a triangle in (T_{h_1}) astride the boundary of the overlap $\Omega_1 \cap \Omega_2$, α_1 and β_1 are piecewise constant over K (see fig. 4a).

On the other hand, if there is no relation of inclusion between the triangles of (T_{h_M}) and (T_{h_1}) in Ω_M, the computation of [36] is unusual. On the example fig. 4b, we see that if the integration is achieved on K_M or K_1, we need to integrate, in the best cases, piecewise polynomia to compute $[\mathrm{B}_1^{K_M\, K_1}]$.

Hence the integrals [34]-[36] present a priori the same numerical treatment difficulty, viz. integrating piecewise polynomia. Without lost of generality, we consider [36] with $\kappa = 0$.

The points and the weight of the quadrature formula we use are respectively denoted by $\hat{\boldsymbol{g}}$ and $\rho_{\hat{\boldsymbol{g}}}$. The finite elements $\{(K, P, \Sigma)\}$ are derived from the reference element $(\hat{K}, \hat{P}, \hat{\Sigma})$ [Cia 78, Bat 90] and we let $\hat{w}_i$, $\boldsymbol{\Phi}_K$ and $|\boldsymbol{d\Phi}_K|$ respectively denote the i-th local shape function in $\hat{K}$, the geometric mapping which transforms $\hat{K}$ into K and the jacobian of $\boldsymbol{\Phi}_K$. We consider K and L, two triangles respectively in (T_{h_M}) and (L_1^K).

$[\mathrm{B}_1^{K\,L}] \leftarrow 0$
↻ $\hat{\boldsymbol{g}}$ sampling point in K
Compute $\tilde{\boldsymbol{g}} = \boldsymbol{\Phi}_L^{-1}(\boldsymbol{\Phi}_K(\hat{\boldsymbol{g}}))$
↻ i degree of freedom associated to K (related local index : I)
↻ j degree of freedom associated to L (related local index : J)
$[\mathrm{B}_1^{K\,L}]_{i\,j} \leftarrow [\mathrm{B}_1^{K\,L}]_{i\,j} + \rho_{\hat{\boldsymbol{g}}}\, \hat{w}_I(\hat{\boldsymbol{g}})\, \hat{w}_J(\tilde{\boldsymbol{g}})\, |\boldsymbol{d\Phi}_K(\hat{\boldsymbol{g}})|$
↺ ↺ ↺

In our case, since we need to integrate piecewise functions, there is no simple accurate integrating formula. The idea lies in judiciously increasing the number of sampling points: given the well-known fact that high degree interpolation polynomials badly approximate piecewise continuous functions, we do not use higher degree polynomial integrating formulae, rather we virtually split the reference element as explained in figure 5.

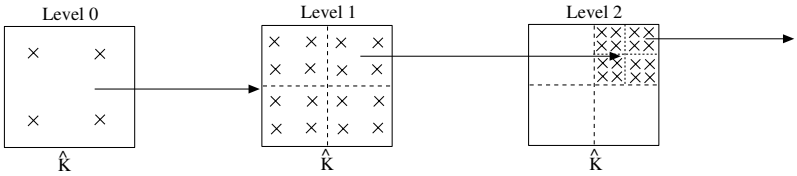

Figure 5. *Hierarchical integrating levels in* $\hat{K}$

Moreover the computation is carried out in a hierarchical way. Namely the error made at the numerical estimation level i can be assessed by comparing the value obtained at the levels i and $i+1$. If the relative difference is greater than a preset threshold, the computation is achieved at a higher level, by considering that we have new integrals to compute on the subelements (4 new integrals for the case considered in figure 5). Though it does not ensure an exact computation, this algorithm gives good results in practice and only a few levels are required in the situations considered in our numerical simulations (see numerical example 4.3).

4. Numerical examples

The use of the internal junction (see fig. 1) presents great potentialities. By judiciously choosing the weight parameter functions, a model can be locally substituted by another one. In this way, one can easily introduce, in a sound model, defects, such as cracks, holes or, at a lower scale, inclusions or voids. Notice that unlike other approaches designed to update a local coarse behaviour of a medium [Ode 97], the *Arlequin* framework allows for this update with a very significant relative gain of flexibility.

4.1. *How to choose the weight parameter functions ?*

The weight parameter functions α_i play a major part when internal junctions are used. In the overlap, outside the glue zone, the two models are superposed but not linked to one another. Therefore the higher the weight function is, the more the associated model *asserts* itself. Accordingly, by choosing very different values for the weight functions, we can activate either of the models and in particular, with a small approximation, we can locally substitute a model for another one.

To illustrate this potentiality, we consider a square plate on which a cracked model is superposed. Given their very different behaviour, we use an internal junction. The glue zone then corresponds to a half ring located at the boundary between the sound model only and the overlap. The left side of the square is clamped and the upper and lower sides are loaded by a symmetric linear pulling effort. The weight vector-valued field $\boldsymbol{\alpha}$ is constant on each elementary subdomain (see subsection 3.1). In figure 6a, we have given weight to the cracked model ($\alpha_{crack} = .999$). In figure 6b, we have chosen $\alpha_{crack} = .001$.

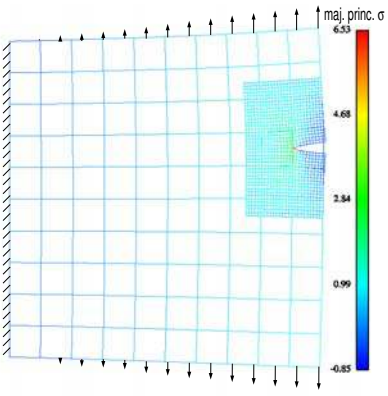

Figure 6a. *Activated crack*

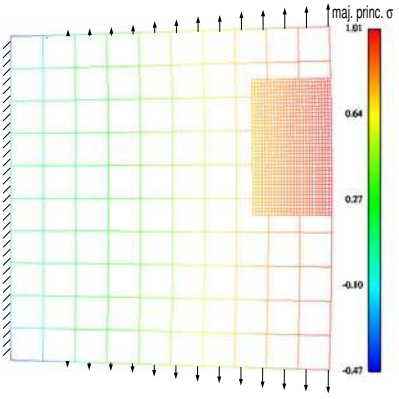

Figure 6b. *Disactivated crack*

By comparing both figures, we notice that the crack is only open in the activated crack case, for which we find a singular stress at the crack tip. In addition, note that this crack can easily (ie. without altering the models) be moved along the right side of the square, which is another major operational advantage of the approach, when compared to more classical ones.

4.2. *How to choose the glue zone ?*

The glue zone stands for the zone where the two models are linked to one another. This zone must therefore be chosen so that the two models are mechanically compatible in it, viz. each of them can represent the mechanical phenomenon we want to simulate. The choice of the glue zone is essential when a defect is introduced in only one element (see numerical example 4.5). To work properly, the defect must be small in relation with the size of the element and the glue zone must be far enough from it, where the related perturbation can be neglected.

4.3. *Need of an elaborated numerical integration*

To illustrate the need to use a somewhat elaborated quadrature strategy, we consider the previous numerical example. The weight is given to the cracked model

($\alpha_{crack} = .999$). In figures 7a and 7b, the deformed meshes and the major principal stresses are represented for different depths of hierarchical integrating levels (see subsection 3.5).

When very few levels are used, we notice that spurious oscillations occur in the glue zone. By adding few levels, those oscillations are suppressed, which shows the efficiency of the integrating strategy used.

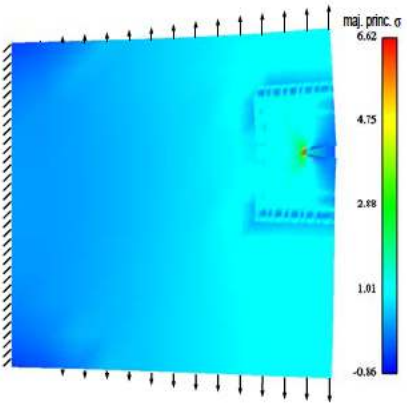

Figure 7a. *One integration level*

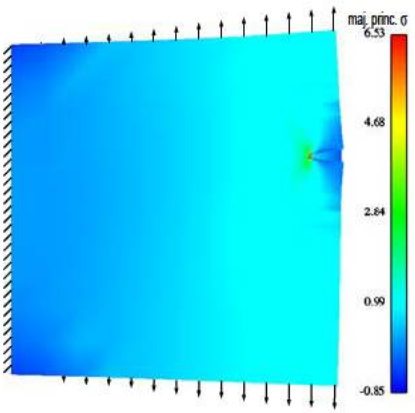

Figure 7b. *Three integration levels*

4.4. *Drilling holes*

To illustrate the possibility of easily *drilling* holes in sound models, we have superposed a holed model on a sound plate loaded by tension forces. The weight vector-valued field $\boldsymbol{\alpha}$ is constant on each elementary subdomain and the holed model is activated ($\alpha_{hole} = .999$). In figure 8a, the resulting deformed meshes and major principal stresses are represented.

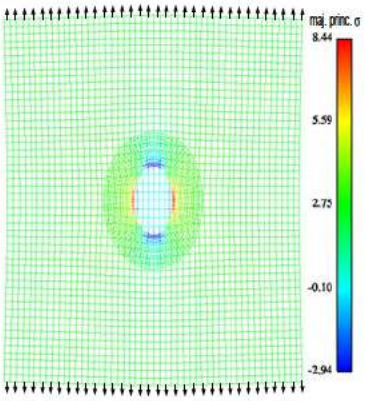

Figure 8a. *Drilling a hole*

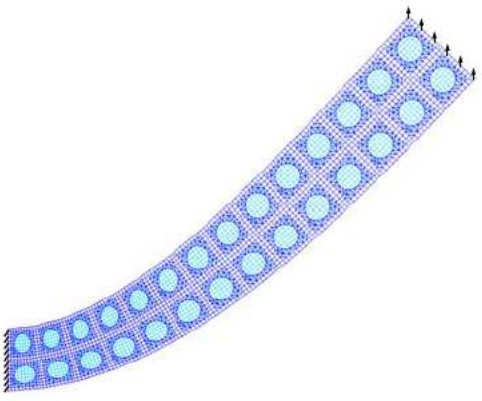

Figure 8b. *Multi-drilled beam*

Note that the stress field is uniform in all the plate except near the notch where the stress concentration ratio is close to the reference [Mus 54] value 3, which shows the efficiency of the method, even with highly incompatible meshes.

This operation can be repeated and a multi-drilled cantilever beam has been modeled in this way. Its free end is submitted to a uniform vertical force. The resulting deformed meshes are represented in figure 8b.

4.5. *Adding inclusions*

We have introduced a model with an inclusion in a sound plate model loaded by compression forces. The idea of substituting models was here carried to extremes, since the inclusion was located in only one element of the sound model. The Young modulus associated to the matrix and the inclusion are respectively 300 and 10000. The weight is given to the inclusion model ($\alpha_{inclusion} = .99$). Figure 9a represents the resulting deformed meshes and the Von Mises field. A zoom on the inclusion is shown in figure 9b.

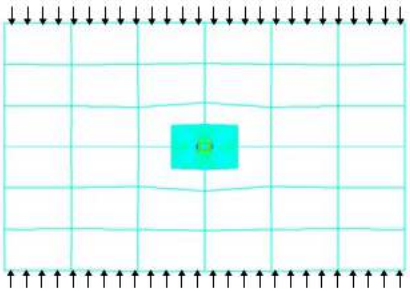

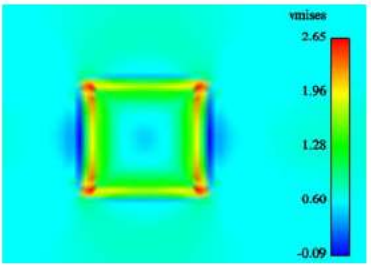

Figure 9a. *Rigid inclusion in one element* **Figure 9b.** *Zoom on the inclusion*

5. Concluding remarks

In this paper, we have detailled the main tools of the *Arlequin* method, focusing in the numerical point of view. In addition, we have carried out some numerical simulations for mechanical problems including general defects. These results illustrate the effectiveness of the approach.

The method is now being implemented in *Code_Aster* developed by Électricité de France. This implementation in a software handling thermo-mechanical non-linear problems should allow us to handle, with a great flexibility, more industrial applications with an appropriate and efficient mechanical and numerical models in the right zone.

6. References

[Bab 00] BABUŠKA I., STROUBOULIS T. AND COPPS K., "The design and analysis of the Generalized Finite Element Method", *Comp. Meth. Appl. Mech. Engrg.*, vol. 181, 2000, p. 43-69.

[Bat 90] BATOZ J-L., DHATT G., "Modélisation des structures par éléments finis", *Hermès, Paris*, , 1990.

[Ben 98] BEN DHIA H., "Multiscale mechanical problems : the Arlequin method", *C.R.Acad.Sci., Paris, Série IIb*, vol. 326, 1998, p. 899-904.

[Ben 99] BEN DHIA. H., "Numerical modelling of multiscale problems : the Arlequin method", *München, ECCM, CD*, , 1999.

[Ben 01a] BEN DHIA H. AND RATEAU G., "Analysis of the Arlequin method and applications to junction problems", *Krakow, ECCM, CD*, , 2001.

[Ben 01b] BEN DHIA H. AND RATEAU G., "Mathematical analysis of the mixed Arlequin method", *C.R.Acad.Sci., Paris, t. 332, Série I*, , 2001, p. 649-654.

[Cia 78] CIARLET P.G., "The finite element method for elliptic problems", *North-Holland, Amsterdam*, , 1978.

[Glo 00] GLOWINSKI R., PAN T-W., HESLA T., JOSEPH D., PERIAUX J., "A distributed Lagrange multiplier/fictitious domain method for the simulation of flow around moving rigid bodies : application to particule flow", *Comp. Mech. Appl. Mech. Engrg.*, vol. 184, 2000, p. 241-267.

[Hug 98] HUGHES T.J.R., FEIJÓO G.R., MAZZEI L. AND QUINCY J-B., "The variational multiscale method - a paradigm for computational mechanics", *Comp. Mech. Appl. Mech. Engrg.*, vol. 138, 1998, p. 3-24.

[Lad 99] LADEVÈZE P. AND DUREISSEIX D., "A new micro-macro computational strategy for structural analysis", *C.R.Acad.Sci., Paris, Série IIb*, vol. 327, 1999, p. 1237-1244.

[Mus 54] MUSKHELISHVILI N.I., "Some basic problems of the mathematical theory of elasticity", *Noordhoff international, Leyden*, , 1954.

[Ode 97] ODEN J.T., ZOHDI T.I., "Analysis and adaptative modelling of highly heterogeneous elastic structures", *Comp. Meth. Appl. Mech. Engrg.*, vol. 148, 1997, p. 367-391.

[Suk 97] SUKUMAR N., MOËS N., MORAN B., BELYTSCHKO T., "Modeling Holes and Inclusions by Level Sets in the eXtended Finite Element Method", *Comp. Meth. Appl. Mech. Engrg.*, vol. 148, 1997, p. 367-391.